

MIT Open Access Articles

Dense transmit and receive antenna arrays

The MIT Faculty has made this article openly available. **Please share** how this access benefits you. Your story matters.

Citation: Wornell, Gregory W. et al. "Dense transmit and receive antenna arrays." Proceedings of the IEEE International Symposium on Antennas and Propagation Society (APSURSI), 2010: 1-4. © 2010 IEEE.

As Published: <http://dx.doi.org/10.1109/APS.2010.5561155>

Publisher: Institute of Electrical and Electronics Engineers (IEEE)

Persistent URL: <http://hdl.handle.net/1721.1/73481>

Version: Final published version: final published article, as it appeared in a journal, conference proceedings, or other formally published context

Terms of Use: Article is made available in accordance with the publisher's policy and may be subject to US copyright law. Please refer to the publisher's site for terms of use.



DENSE TRANSMIT AND RECEIVE ANTENNA ARRAYS

C.-P. Yeang*¹, G. W. Wornell², L. Zheng², and J. Krieger²

¹ IHPST, Univ. Toronto, ON, Canada

² Dept. EECS, MIT, Cambridge, MA, USA

E-mail: chenpang.yeang@utoronto.ca

Introduction

Recent progress in millimeter-wave and microwave integrated circuit (IC) manufacturing technology has created new opportunities for the development of novel, low-cost antenna array architectures. In such systems, the associated specifications on RF components such as phase-shifters, oscillators, and amplifiers, can be challenging to meet in a cost-effective manner. In this paper, we develop a dense antenna array to ease such RF circuit requirements without sacrificing performance, and demonstrate its effectiveness for transmit and receive beamforming. We also investigate the effects of mutual coupling and impedance matching on the system performance.

The Traditional Array Architecture

In a traditional uniform linear array, an aperture of length L is formed from a collection of antenna elements, adjacent pairs of which are spaced d apart. The nominal spacing between elements is $d = \lambda/2$. Provided that elements are at least as close as this nominal spacing, the maximum number of available degrees of freedom offered by the aperture can be realized, and, in phased-array applications in particular, grating lobes in beamforming patterns can be avoided. Thus, since $L = (N - 1)d$, the minimum number of antenna elements required is typically $N_o = 1 + 2L/\lambda$.

With the associated antenna array architecture, a beam pattern can be formed by choosing antenna element weights $w_n = a_n e^{j\theta_n}$. This is implemented via N amplitude attenuators and N phase shifters. At the transmitter, the RF signal passes through such a beamformer, whose N outputs are directed to N power amplifiers and then N antennas. At the receiver, the N antenna signals that result from the incoming wave pass through N low-noise amplifiers, are phase-shifted, amplitude-adjusted, and superimposed via the beamformer to form the output signal. The associated transmitter and receiver array radiation patterns are, respectively,

$$B^{\text{T,R}}(\psi) = \left| \sum_{n=1}^N w_n e^{\mp jnk d \cos \psi} \right|, \quad (1)$$

where $k = 2\pi/\lambda$ is the wave number and ψ is the target angle of radiation.

The traditional array architecture poses challenges to circuit design and device technology. Accuracy of the array radiation patterns in (1) depends on the accuracy with which $\{\theta_n\}$ and $\{a_n\}$ are implemented. This implies that the phase shifters in the beamformers must be implemented with high resolution. Moreover, the power

amplifiers at the transmitter must have high linearity. Although a variety of approaches have been proposed to improve the precision of these components, most remain expensive and complicated; see, e.g., [1-3].

An Oversampling Array Architecture

In contrast with the traditional architecture, we consider packing *more* antennas N in the given aperture than would otherwise be required, i.e., $N > N_o$, for both transmit and receive array configurations. This density is then exploited in a manner analogous to the way temporal oversampling is exploited in data converter design. In particular, just as sampling at a rate exceeding that dictated by the Nyquist criterion reduces quantization resolution requirements, the dense array uses N lower-quality RF components instead of N_o higher quality ones.

To reduce our RF component specifications, we constrain our system to use coarsely quantized versions of the weights w_n , and exploit the oversampling to minimize the effect of such quantization. In particular, we exploit the principle of $\Delta\Sigma$ quantization [4] by directly translating it to the spatial domain.

The spatial $\Delta\Sigma$ architecture is depicted in Fig. 1, and involves creating a sequence of quantized weights v_n that “act” in a manner asymptotically indistinguishable from the desired weights w_n . The associated processing proceeds as follows. At the n th antenna, we obtain the difference between the input of the $(n - 1)$ th quantizer and v_{n-1} at the output of the $(n - 1)$ th quantizer, corresponding to the Δ part of the structure. We then add that difference to the desired weight w_n , corresponding to the Σ part of the structure. The result is then quantized using 4-PSQ (phase-shift quantization, where the input is quantized to a constant amplitude and one of four phases: $0^\circ, 90^\circ, 180^\circ, 270^\circ$), which corresponds to quantizing each of the in-phase and quadrature components to a single bit. As such only crude 4-angle phase shifters and (nonlinear) bilevel power amplifiers are required in the RF front-end.

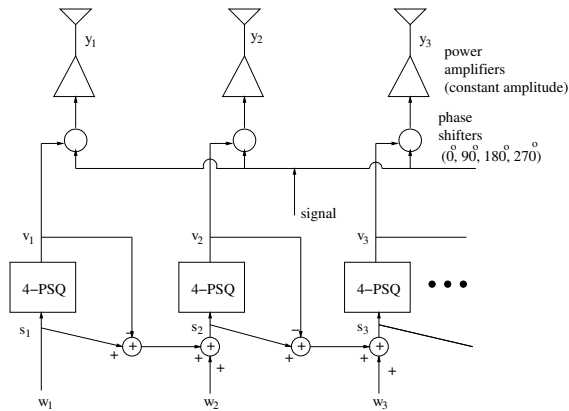


Figure 1: The spatial $\Delta\Sigma$ architecture at the transmitter. The corresponding receiver architecture is obtained by reversing the beamformer to have multiple inputs and a single output, i.e., the n th antenna input from the low-noise amplifier is mixed with v_n , then all such terms are summed.

Error Analysis for Spatial $\Delta\Sigma$

Spatial $\Delta\Sigma$ oversampling can be understood in a manner analogous to the way traditional temporal $\Delta\Sigma$ oversampling is understood. In the latter, a time series $\{w_n\}$ is quantized into another time series $\{v_n\}$, from which one can recover $\{w_n\}$ by low-pass filtering. That recovery is possible follows from the fact that the feedback structure of $\Delta\Sigma$ forces the average value of the quantized output to track the average input, which has the advantage of suppressing the quantization error spectrum at low frequencies. Similar behavior takes place in the case of our spatial $\Delta\Sigma$ scheme. To see how the associated spatial low-pass filtering arises, note that the transmit and receive array patterns $B^T(\psi)$ and $B^R(\psi)$ in (1) are effectively the Fourier transforms of the weights $\{w_n\}$ or $\{v_n\}$ at the spatial frequency $\omega = \pm kd \cos \psi = \pm kL \cos \psi / (N - 1)$. Hence, $\omega \rightarrow 0$ as $N \rightarrow \infty$, i.e., the beamforming operation itself provides the required spatial low-pass filtering.

Ignoring mutual coupling between antennas for the moment, one can show formally that (for transmit arrays)

$$\hat{B}^T(\psi) - B^T(\psi) = O\left(\frac{1}{\sqrt{N}}\right), \quad (2)$$

where $\hat{B}^T(\psi) = \left| \sum_{n=1}^N v_n e^{-jnk d \cos \psi} \right|$. The corresponding receive array expressions $\hat{B}^R(\psi) - B^R(\psi)$ are obtained by replacing j with $-j$.

Equation (2) can be derived by expressing v_n in terms of the sum of w_n and the differential quantization error $e_n - e_{n-1}$. The difference between $\hat{B}^T(\psi)$ and $B^T(\psi)$ becomes $(1 - e^{-jkd \cos \psi}) \times \sum_{n=1}^N e^{-jnk d \cos \psi} \tilde{e}_n$ that can be shown to be in the order of $1/\sqrt{N}$ for large N . Under the $\Delta\Sigma$ oversampling array scheme, therefore, the radiation patterns from the quantized excitations converge asymptotically to those from the original, finer excitations with an increasing number of antennas.

In a more refined analysis, we include the effects of both antenna mutual coupling and impedance matching. We use the EMF method to compute the array's self and mutual impedances [5]. We also examine the effect of a scan-impedance matching network fixed at the average antenna excitation (see next section).

Simulation Results

In this section, we present some simulation results. The parameters are set as follows: The wavelength is $\lambda = 3$ cm (frequency 10 GHz). The uniform 1-D array has overall length $L = 5\lambda = 15$ cm. Each cylindrical antenna has length $l_a = 1$ cm and radius $r_a = 1$ mm. The signal-feeding transmission lines have characteristic impedance $R_0 = 50$ ohm, length $l_t = 0.8\lambda = 2.4$ cm, and attenuation $\alpha_t = 5.0/\text{m}$. The angular range for beamforming is $\psi \in [0, \pi]$. The matching network is based on the scan impedances for uniform excitations at the transmitter and the receiver.

We compute the array pattern error $\|\hat{B} - B\|$ averaged over the looking angle and separable patterns when the antenna mutual coupling and the matching network are

incorporated. In Fig. 2(a), we present the numerical results for the transmit phased array under three conditions: scan-impedance matching, no impedance matching, and no antenna mutual coupling. The curve without mutual coupling demonstrates the sheer effect of $\Delta\Sigma$ quantization error, which diminishes toward 0 with N as asserted previously. Although antenna mutual coupling does incur some penalty in convergence rate of the beam pattern quantization error, the benefits of oversampling are still apparent.

We can reach the same conclusion for a receive array. Fig. 2(b) shows the receive array pattern errors with respect to N . We compare the case in which the scan-impedance matching and antenna mutual coupling are taken into account with the default case in which none of the two effects are present. Again, the figure shows the benefit of oversampling, in spite of mutual coupling and scan-impedance matching.

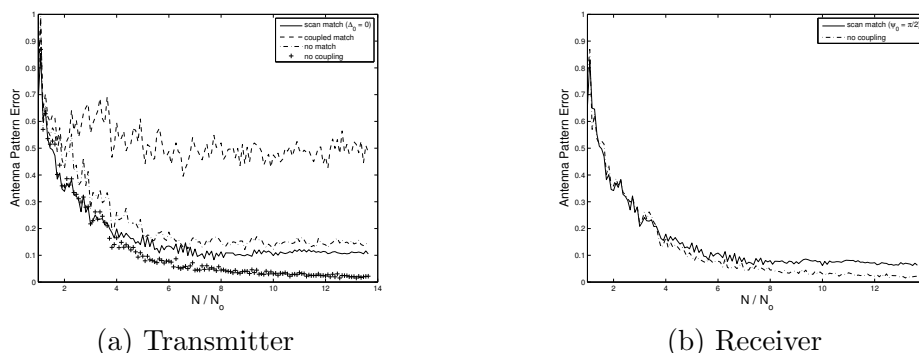


Figure 2: The array-pattern error at the transmitter and receiver. (Phased array. With and without mutual coupling and impedance matching.)

References

- [1] D. Parker and D. C. Zimmermann, “Phased arrays—Part II: Implementations, applications, and future trends,” *IEEE Trans. Microwave Theory, Techniques*, vol. 50, pp. 688–698, Mar. 2002.
- [2] J. Roderick, H. Krishnaswamy, K. Newton, and H. Hashemi, “Silicon-based ultra-wideband beam-forming,” *IEEE J. Solid-State Circuits*, vol. 41, pp. 1726–1739, Aug. 2006.
- [3] H. Hashemi, X. Guan, A. Komijani, and A. Hajimiri, “A 24-GHz SiGe phased-array receiver—LO phase-shifting approach,” *IEEE Trans. Microwave Theory, Techniques*, vol. 53, pp. 614–626, Feb. 2005.
- [4] S. R. Norsworthy, R. Schreier, and G. C. Temes, *Delta-Sigma Data Converters: Theory, Design, and Simulation*, New York: IEEE Press, 1997.
- [5] R. W. P. King, G. J. Fikioris, and R. B. Mack, *Cylindrical Antennas and Arrays*, Cambridge: Cambridge University Press, 2002.